BLOCK ADJUSTMENT WITH RATIONAL POLYNOMIAL CAMERA MODELS

Gene Dial
Product Engineering Manager
Jacek Grodecki
Photogrammetric Systems Engineering Manager
Space Imaging LLC
12076 Grant Street
Thornton, Colorado 80241
gdial@spaceimaging.com
jgrodecki@spaceimaging.com

ABSTRACT

Rational Polynomial Camera (RPC) models transform 3-dimensional object space coordinates into 2-dimensional image coordinates. RPC models are simple, fast, and accurate. Traditional photogrammetric workflows perform block adjustment with a physical camera model and then calculate RPC coefficients to speed the terrain extraction, orthorectification, and feature extraction tasks. RPC coefficients provide a simple, compact means of communicating camera object-image relations from image data provider to image data user. What has been lacking is a method to use ground control and other controlled imagery to improve the accuracy of imagery described by RPC coefficients. Previous attempts to block adjust imagery described by RPC models have failed due to the complexity of adjusting the 78 coefficients inherent in an RPC model. Even if RPC block adjustment were successful, users might object that RPC coefficients do not directly relate to camera exterior and interior orientation parameters and so do not provide insight into the geometric properties being adjusted. Contrary to this previous experience, the authors have found that it is possible to block adjust imagery with RPC models by adding an adjustment model with parameters directly related to geometric properties. Multiple physical parameters having the same net effect on the object-image relationship are combined into a single adjustment parameter. Consequently, the proposed method is numerically more stable than traditional adjustment of physical camera parameters. This paper describes how to block adjust imagery described by an RPC model and illustrates that method with results processing IKONOS satellite imagery.

BACKGROUND

Satellite Imagery

The launch of IKONOS on September 24, 1999 heralded a new era of commercially available, high-resolution satellite imagery. Overviews of the IKONOS satellite may be found in (Dial 2001 and Dial et. al. 2001).

Photogrammetric processing of satellite image can however be more complicated than aerial camera processing. Aerial cameras acquire an image at an instant of time with a unique exposure station and orientation. Many satellite cameras (including IKONOS) use linear sensor arrays that scan an image strip while the satellite orbits. Consequently the satellite image is acquired over a period of time so that the exposure station and orientation are also functions of time. (See figure 1). The master document describing the IKONOS camera model is 183 pages long. It requires a supplementary document describing ephemeris, attitude, and calibration data formats in another 225 pages. The complexity of transmitting, implementing, and testing mathematical models has led Space Imaging to hold private the detailed mathematical description of the IKONOS camera. That approach has however frustrated some image applications requiring a detailed description of the object-to-image relationship available from a complete camera model.

RPC Geometry

To meet the need to provide the object-image relationship with its images, Space Imaging provides an Image Geometry Model (IGM) in RPC (Rational Polynomial Coefficient) format with ortho-kit and stereo image products. All images ordered together are block adjusted together in the ground station and RPC data is calculated to accurately describe the object-image relationship resulting from that block adjusted imagery. With RPC data, users can do point positioning, vector extraction, and DEM (Digital Elevation Model) generation from stereo images. The ortho-kit images, comprising a mono image taken from a high elevation angle and RPC data, can be orthorectified with a suitable DEM. Exact equations and format can be found in (Dial, 2000), a document of only 5 pages including examples. RPC data thus provides a mathematical equation that simply and accurately describes the object-image relationship.

RPC Block Adjustment

While RPC data has extended the utility of IKONOS images to permit feature extraction and orthorectification, that data has not heretofore provided the means for users to perform their own photogrammetric block adjustment. While Space Imaging originally envisioned all block adjustment being performed in its ground station, ensuring consistent quality of results, we have been confronted by a reality that some customers have proprietary ground control or controlled imagery that cannot be handled in our ground station. Meeting the needs of those customers required a method for them to block adjust their data outside the ground station. Economic incentives have led other investigators to propose various methods for photogrammetric processing of IKONOS images (Toutin & Cheng 2000). Those investigators have been hampered by lack of incomplete knowledge of the IKONOS camera model, of the maneuvering possible during image acquisition, and by limited availability of generally expensive test data sets. This publication of a technique for block adjusting IKONOS images described by RPC data is motivated by a desire to ensure that IKONOS images are processed in such way as to achieve consistently accurate results for quality purposes and is further motivated by a desire to satisfy clients needing to do their own block adjustment. In developing the adjustment model described here, the authors had access to the complete description of IKONOS imaging geometry, familiarity with all of the satellite maneuvering modes, the resources of extensive test ranges and imagery with which to test and validate, and the experience gained calibrating, testing, and troubleshooting IKONOS metric projects.

THE IKONOS CAMERA MODEL

To develop this method of RPC block adjustment, the authors began by considering the geometric properties of IKONOS images. The IKONOS camera model involves typical elements of interior and exterior orientation.

Interior Orientation

Interior orientation includes parameters for detector positions, principal point, optical distortion, and focal length. Unlike film cameras, the IKONOS digital focal plane does not require fiducial marks. Instead, every pixel is at a fixed, calibrated position on the solid-state focal plane. The detectors are rigidly attached to the focal plane in a stable thermal-mechanical environment. The elements of interior orientation can be determined to exquisite accuracy with well-controlled test-range imagery. Consequently it is not necessary, indeed it is not desirable, to adjust the interior orientation during standard imaging operations. Accurately calibrated digital cameras can simplify photogrammetric block adjustment by removing interior orientation parameters from the block adjustment process.

Exterior Orientation

Exterior orientation comprises position and attitude. On-board GPS receivers determine the satellite ephemeris, i.e., camera position as a function of time. Ephemeris errors are called in-track, cross-track, and radial. Star trackers and gyros determine attitude as a function of time. Attitude angles are roll (rotation about the in-track direction), pitch (rotation about the cross-track direction), and yaw (rotation about the radius from the center of the Earth).

Ephemeris and attitude have finite accuracy, about one meter for ephemeris and about one or two arc-seconds for attitude. From an orbital altitude of 680km, one arc-second of attitude error results in 3.3 meters horizontal position error at nadir or proportionately more as the slant-range increases for off-nadir images, so attitude adjustment is important to the block-adjustment process. Before adjusting 3 parameters of position and another 3 parameters of attitude, we considered first the effects of these parameters on the object-image relationship and found (1) that in-track and cross-track position errors are completely correlated with pitch and roll attitude errors so that they cannot be separately estimated (2) that yaw errors are negligible, and (3) that radial errors are so small as to be negligible too. Thus it is only necessary to estimate roll and pitch. These conclusions may be somewhat startling so we will take some time and space to illustrate these points.

Attitude Errors. Because the star trackers are approximately perpendicular to each other, satellite roll, pitch, and yaw are all known with about equal accuracy. The slant range from the satellite to the ground magnifies the effect of roll or pitch by the slant-range from satellite to ground, a distance of 680km or more. Thus an arc-second error of roll or pitch causes 3.3m or more displacement on the ground. The situation with yaw is different. (See figure 2). The ground displacement due to a yaw error is that error multiplied by half the swath width. For a yaw error of 2" and swath width of 11 km, the ground displacement is only 0.055 meters, a negligible amount. Thus roll and pitch errors are significant but yaw errors are negligible.

Ephemeris Errors. Ephemeris errors are conventional separated into in-track, cross-track, and radial ephemeris errors. We will first show that in-track and cross-track errors are equivalent to pitch and roll attitude errors. Then we will show that radial errors are negligible.

In-track and Cross-track Ephemeris Errors. For narrow field of view cameras, small horizontal displacements are equivalent to small angular rotations. Figure 3 shows one camera in a nominal, nadir-pointing attitude and another camera displaced to the right but rotated to the left so that its principal point images the same ground point.

For example, lets assume a roll error of 2" with the camera displaced horizontally by an equivalent amount d = 6.593466m. Compared to the original nadir-pointing camera, the displaced and rotated camera differs in the edges of the field of view by X1 – X1' = X2 – X2' = 0.000454m. The difference between the nominal camera and another camera that has been rotated and correspondingly displaced is absolutely negligible, less than 1/2000 pixel. We could complicate the argument by including effects of an off-nadir nominal attitude and the curvature of the earth, but the effect would be the same, that for any exterior orientation error could be equivalently represented with attitude only or ephemeris only.

Radial Ephemeris Errors. The above addresses the equivalence of in-track and cross-track ephemeris errors with attitude pitch and roll. Radial ephemeris errors result in scale errors. A 1m radial error of a 680km orbit height causes a 1.5ppm scale factor error that causes a 16mm positioning error across the ~11km swath width. Radial error effects are thus negligible for IKONOS.

Drift Errors. While attitude and ephemeris errors are largely biases, there exists the possibility that these errors would drift as a function of time. For example, gyro errors without sufficient compensation from the star trackers could introduce an error in attitude rate. These errors have been found to be small, less than 0.1 pixel per 100 km, and so are largely negligible.

Required Adjustments. High resolution satellite imaging systems necessarily have a narrow angle field of view. The narrow field of view results in almost complete correlation of parameters dealing with satellite position and attitude. While wide field of view aerial cameras have sufficient distortion to distinguish angular rotations from linear translations, narrow field of view satellite cameras do not.

Having said that so many effects are negligible or completely correlated with other effects, the reader may question what actually must be adjusted. We have found that it comes down to this: one parameter is required to adjust for errors in the line direction and another parameter is required to adjust for errors in the sample direction. The line parameter absorbs effects of orbit, attitude, and residual interior orientation errors in the line direction. The sample parameter absorbs the same effects in the sample direction. Parameters for drift can be added but in our experience are not generally required.

RPC CAMERA MODEL

The Rational Polynomial Camera (RPC) model and techniques for determining its coefficients have previously been described in (Grodecki 2001) and (Grodecki & Dial 2001) but will also be briefly summarized here. The RPC model relates the object space (*Latitude, Longitude, Height*) coordinates to image space (*Line, Sample*) coordinates. The RPC functional model is of the form of a ratio of two cubic functions of object space coordinates. Separate rational functions are used to express the object space to line and the object space to sample coordinate relationships.

Given the WGS84 object space coordinates (*Latitude, Longitude, Height*), where *Latitude* is geodetic latitude expressed in degrees, *Longitude* is geodetic longitude expressed in degrees, and *Height* is height above the WGS84 ellipsoid in meters, the calculation of image space coordinates begins by normalizing latitude, longitude, and height as follows:

$$P = \frac{Latitude - LAT\_OFF}{LAT\_SCALE} \qquad (1)$$

$$L = \frac{Longitude - LONG\_OFF}{LONG\_SCALE} \qquad (2)$$

$$H = \frac{Height - HEIGHT\_OFF}{HEIGHT\_SCALE} \qquad (3)$$

The normalized *Line* and *Sample* image space coordinates (Y, X) are then calculated from their respective rational polynomial functions *f(.)* and *g(.)* as

and

$$Y = f(Latitude, Longitude, Height) = \frac{Num_L(P,L,H)}{Den_L(P,L,H)} \qquad (4)$$

where

$$\begin{aligned} Num_L(P,L,H) = {} & a_1 + a_2 \cdot L + a_3 \cdot P + a_4 \cdot H + a_5 \cdot L \cdot P + a_6 \cdot L \cdot H + a_7 \cdot P \cdot H + a_8 \cdot L^2 + a_9 \cdot P^2 \\ & + a_{10} \cdot H^2 + a_{11} P \cdot L \cdot H + a_{12} \cdot L^3 + a_{13} \cdot L \cdot P^2 + a_{14} \cdot L \cdot H^2 + a_{15} \cdot L^2 \cdot P + a_{16} \cdot P^3 + a_{17} \cdot P \cdot H^2 \qquad (5) \\ & + a_{18} \cdot L^2 \cdot H + a_{19} \cdot P^2 \cdot H + a_{20} \cdot H^3 \end{aligned}$$

$$\begin{aligned} Den_L(P,L,H) = {} & 1 + b_2 \cdot L + b_3 \cdot P + b_4 \cdot H + b_5 \cdot L \cdot P + b_6 \cdot L \cdot H + b_7 \cdot P \cdot H + b_8 \cdot L^2 + b_9 \cdot P^2 \\ & + b_{10} \cdot H^2 + b_{11} P \cdot L \cdot H + b_{12} \cdot L^3 + b_{13} \cdot L \cdot P^2 + b_{14} \cdot L \cdot H^2 + b_{15} \cdot L^2 \cdot P + b_{16} \cdot P^3 + b_{17} \cdot P \cdot H^2 \qquad (6) \\ & + b_{18} \cdot L^2 \cdot H + b_{19} \cdot P^2 \cdot H + b_{20} \cdot H^3 \end{aligned}$$

$$X = g(Latitude, Longitude, Height) = \frac{Num_S(P,L,H)}{Den_S(P,L,H)} \qquad (7)$$

where

$$\begin{aligned} Num_S(P,L,H) = {} & c_1 + c_2 \cdot L + c_3 \cdot P + c_4 \cdot H + c_5 \cdot L \cdot P + c_6 \cdot L \cdot H + c_7 \cdot P \cdot H + c_8 \cdot L^2 + c_9 \cdot P^2 \\ & + c_{10} \cdot H^2 + c_{11} P \cdot L \cdot H + c_{12} \cdot L^3 + c_{13} \cdot L \cdot P^2 + c_{14} \cdot L \cdot H^2 + c_{15} \cdot L^2 \cdot P + c_{16} \cdot P^3 + c_{17} \cdot P \cdot H^2 \qquad (8) \\ & + c_{18} \cdot L^2 \cdot H + c_{19} \cdot P^2 \cdot H + c_{20} \cdot H^3 \end{aligned}$$

$$\begin{aligned} Den_S(P,L,H) = {} & 1 + d_2 \cdot L + d_3 \cdot P + d_4 \cdot H + d_5 \cdot L \cdot P + d_6 \cdot L \cdot H + d_7 \cdot P \cdot H + d_8 \cdot L^2 + d_9 \cdot P^2 \\ & + d_{10} \cdot H^2 + d_{11} P \cdot L \cdot H + d_{12} \cdot L^3 + d_{13} \cdot L \cdot P^2 + d_{14} \cdot L \cdot H^2 + d_{15} \cdot L^2 \cdot P + d_{16} \cdot P^3 + d_{17} \cdot P \cdot H^2 \qquad (9) \\ & + d_{18} \cdot L^2 \cdot H + d_{19} \cdot P^2 \cdot H + d_{20} \cdot H^3 \end{aligned}$$

The de-normalized image space coordinates (*Line, Sample*), where *Line* is image line number expressed in pixels with zero at the center of the upper-most line, and *Sample* is sample number expressed in pixels with zero at the center of the left-most sample are finally computed as

$$Line = Y \cdot LINE\_SCALE + LINE\_OFF \qquad (10)$$

$$Sample = X \cdot SAMP\_SCALE + SAMP\_OFF \qquad (11)$$

The 78 required coefficients, $\{a_1 \ldots a_{20}, b_2 \ldots b_{20}, c_1 \ldots c_{20}, d_2 \ldots d_{20}\}$, can be determined by fitting the physical camera model as described in the next section and are supplied with ortho-kit and stereo images. Given these coefficients, the computation of (*Line*, *Sample)* is fast and easy.

DETERMINING RPC COEFFICIENTS

A least-squares approach is utilized to estimate the RPC model coefficients a_i, b_i, c_i, and d_i from a 3-dimensional grid of points generated using a physical camera model (see Figure 4). As pointed out in (Hu & Tao, 2001) attempts to use ground control only to determine RPC coefficients (Tao & Hu, 2001) risks numerical instability during the fitting process and poor compliance with camera physics. RPC coefficients determined by fitting a 3-dimensional grid of object points to conjugate image points generated with the physical camera model result in a very accurate fit with 0.01 pixel σ or 0.04 pixel worst case (Grodecki 2001).

RPC BLOCK ADJUSTMENT MODEL

The RPC block adjustment math model proposed in this paper is defined in the image space. It uses denormalized *a priori* rational polynomial camera (RPC) model, p and r, as defined by the functions f and g to express the object space to image space relationship. The adjustable functions, Dp and Dr, are added to the *a priori* rational functions to capture the discrepancies between the *a priori* and the measured image space coordinates. Each image has its own set of RPC coefficients to describe the geometry of that individual image.

The RPC Block Adjustment math model, for the *k-th* ground control or tie point being the *i-th* image point on the *j-th* image, is thus defined as follows:

$$Line_i^{(j)} = \Delta p^{(j)} + p^{(j)}\left(Latitude_k, Longitude_k, Height_k\right) + e_{Lij} \quad (12)$$

$$Sample_i^{(j)} = \Delta r^{(j)} + r^{(j)}\left(Latitude_k, Longitude_k, Height_k\right) + e_{Sij} \quad (13)$$

where

$Line_i^{(j)}$ and $Sample_i^{(j)}$ are measured (on image j) line and sample coordinates of the *k-th* ground control or tie point with object space coordinates ($Latitude_k$, $Longitude_k$, $Height_k$),

$\Delta p^{(j)}$ and $\Delta r^{(j)}$ are the adjustment terms expressing the differences between the measured and the nominal line and sample coordinates of ground control and/or tie points, for image j,

e_{Lij} and e_{Sij} are random unobservable errors, and

$p^{(j)}$ and $r^{(j)}$ are the given line and sample, denormalized RPC models for image j:

$$p\left(Latitude, Longitude, Height\right) = f\left(Latitude, Longitude, Height\right) \cdot LINE\_SCALE + LINE\_OFF \quad (14)$$

$$r\left(Latitude, Longitude, Height\right) = g\left(Latitude, Longitude, Height\right) \cdot SAMPLE\_SCALE + SAMPLE\_OFF$$

(15).

We are proposing to use a polynomial model defined on the domain of image coordinates to represent the adjustable functions, Dp and Dr.

$$\Delta p = a_0 + a_S \cdot Sample + a_L \cdot Line \quad (16)$$

$$\Delta r = b_0 + b_S \cdot Sample + b_L \cdot Line \quad (17)$$

The choice of the image coordinate system to define the adjustable functions is influenced by the need to tie the adjustable model to the physics of the imaging operation. A polynomial model is simple, linear in adjustment parameters, yet flexible enough to accurately model the IKONOS sensor.

Each of the parameters in the above has physical significance. Parameter a_0 absorbs all in-track effects causing offsets in the line direction including in-track ephemeris, satellite pitch attitude, cross-array principal point and cross-array detector positions. As discussed earlier, for narrow field of view instruments with strong a-priori, all of these physical parameters have the same net effect of displacing images in line. Similarly, parameter b_0 absorbs all cross-track effects causing offsets in the sample direction including cross-track ephemeris, satellite roll attitude, along-array principal point and along-array detector positions. Because the line direction is equivalent to time, parameters a_L and b_L absorb the small effects due to gyro drift during the imaging scan. Parameters a_L and b_L turn out to only be required for images that are 100km or longer.

EVALUATION OF IMAGE SPACE ADJUSTMENTS TO THE RPC MODEL

The following image space adjustment models were tested by simulation:

(1) $\Delta p = a_0 + a_S \cdot Sample + a_L \cdot Line$

(2) $\Delta p = a_0 + a_L \cdot Line$

(3) $\Delta p = a_0 + a_S \cdot Sample$

(4) $\Delta p = a_0$

and

(5) $\Delta r = b_0 + b_S \cdot Sample + b_L \cdot Line$

(6) $\Delta r = b_0 + b_L \cdot Line$

(7) $\Delta r = b_0 + b_S \cdot Sample$

(8) $\Delta r = b_0$

where

$a_0, b_0, a_L, b_L, a_S, b_S$ are the image adjustment parameters, and
Line, *Sample* are the line and sample coordinates of a ground control (or tie) point.

The differences (ΔL, ΔS) between the original and the perturbed image coordinates were subsequently calculated, and used as input to the tested adjustment models.

For each of the tested RPC Block Adjustment models the adjustment parameters (a_0, b_0, a_L, b_L, a_S, b_S) were estimated using the least-squares approach. The post-fit RMS errors and the maximum residual errors were then computed for each of the models.

A number of scenarios were generated for this purpose — using the following ranges of scanning azimuth, roll and pitch angles, and geographic location:

- Roll (0^o, 10^o, 20^o, 30^o)
- Pitch (0^o, 10^o, 20^o, 30^o)
- Azimuth (0^o, 45^o, 90^o, 135^o, 180^o, 225^o, 270^o, 315^o)
- Latitude (0^o, 30^o, 60^o)

The image strip length was varied from 10 km to 100 km. The minimum elevation angle was set to 50 degrees.

The errors in the ephemeris and attitude were set to:

- 3 meters in the ephemeris components (in-track, cross-track, and radial)
- 2” in the attitude angles (pitch, roll, yaw)

Figure 5 illustrates the process of simulating imaging scenarios, camera perturbations, adjustment model fitting, and evaluation leading to the results that will now be described.

Maximum residual and RMS errors, from all imaging scenarios, were computed giving the measure of the worst possible math model errors when using the proposed RPC Block Adjustment approach. The results of the analysis are shown below.

Strip Length	Adjustment model	Max residual sample error [pixels]	Max RMS sample error [pixels]	Max residual line error [pixels]	Max RMS line error [pixels]
10 km	$\Delta p = a_0$ $\Delta r = b_0$	0.21	0.10	0.21	0.09
	$\Delta p = a_0 + a_L \cdot Line$ $\Delta r = b_0 + b_L \cdot Line$	0.15	0.10	0.12	0.08
	$\Delta p = a_0 + a_S \cdot Sample$ $\Delta r = b_0 + b_S \cdot Sample$	0.09	0.06	0.10	0.07
	$\Delta p = a_0 + a_S \cdot Sample + a_L \cdot Line$ $\Delta r = b_0 + b_S \cdot Sample + b_L \cdot Line$	0.004	0.001	0.001	0.001
20 km	$\Delta p = a_0$ $\Delta r = b_0$	0.28	0.13	0.32	0.15
	$\Delta p = a_0 + a_L \cdot Line$ $\Delta r = b_0 + b_L \cdot Line$	0.15	0.10	0.12	0.08
	$\Delta p = a_0 + a_S \cdot Sample$ $\Delta r = b_0 + b_S \cdot Sample$	0.19	0.12	0.22	0.13
	$\Delta p = a_0 + a_S \cdot Sample + a_L \cdot Line$ $\Delta r = b_0 + b_S \cdot Sample + b_L \cdot Line$	0.01	0.002	0.004	0.001
50 km	$\Delta p = a_0$ $\Delta r = b_0$	0.57	0.29	0.66	0.34
	$\Delta p = a_0 + a_L \cdot Line$ $\Delta r = b_0 + b_L \cdot Line$	0.16	0.10	0.13	0.08
	$\Delta p = a_0 + a_S \cdot Sample$ $\Delta r = b_0 + b_S \cdot Sample$	0.50	0.28	0.58	0.33
	$\Delta p = a_0 + a_S \cdot Sample + a_L \cdot Line$ $\Delta r = b_0 + b_S \cdot Sample + b_L \cdot Line$	0.02	0.01	0.02	0.01
100 km	$\Delta p = a_0$ $\Delta r = b_0$	1.00	0.51	1.25	0.66
	$\Delta p = a_0 + a_L \cdot Line$ $\Delta r = b_0 + b_L \cdot Line$	0.17	0.10	0.17	0.08
	$\Delta p = a_0 + a_S \cdot Sample$ $\Delta r = b_0 + b_S \cdot Sample$	0.93	0.50	1.17	0.65
	$\Delta p = a_0 + a_S \cdot Sample + a_L \cdot Line$ $\Delta r = b_0 + b_S \cdot Sample + b_L \cdot Line$	0.07	0.03	0.06	0.03

These simulations show that the postulated adjustment models can accurately absorb the effects of ephemeris and attitude errors. Bias only models (parameters a_0 and b_0 only) are effective for strip lengths up to 50km. Strips of 100km length may require the addition of drift parameters (a_L and b_L) for full accuracy. Parameters proportional to sample (a_S and b_S) and higher order terms are not normally required.

EXPERIMENTAL RESULTS

A Space Imaging project with 6 stereo strips and a large number of Ground Control Points (GCP) as shown in figure 6 was selected to demonstrate the technique. Each of the 12 source images was produced as a georectified image with RPC data from stereo images that any customer might order. The images were then loaded onto a SOCET SET® workstation running a Space Imaging developed "camera" model with RPC coefficients and a choice of a 2 to 6 parameter adjustment model. Tie points were positioned along the edges of the images. Ground points were selectively changed between control and check points to produce the results shown. The results presented here will use a simple two-parameter, image-space bias only model with *a priori* values of zero and sigma of 10 pixels.

Experimental results are summarized in the table below.

GCP	Avg. X	Avg. Y	Avg Z	StDev X	StDev Y	StDev Z	CE90
None	-5.0	6.2	1.6	0.97	1.08	2.02	8.2
1 in center	-2.4	0.5	-1.1	0.95	1.07	2.02	3.3
3 on edge	-0.4	0.3	0.2	0.97	1.06	1.96	2.2
4 in corners	-0.2	0.3	0.0	0.95	1.06	1.95	2.2
All	0.0	0.0	0.0	0.55	0.75	0.50	1.4

Horizontal residual errors are plotted in figures 7 to 11.

The average errors without control were (-5, 6, 2) meters in (X, Y, Z). This illustrates IKONOS accuracy without ground control. The addition of one ground control point reduces the average error to (-2, 1, -1) meter, viz., the error of reading that GCP. Additional ground control further reduces the average error. The standard deviation about the average is 1 meter in X and Y and 2 meters in Z. This standard deviation does not appreciably reduce until all 40 control points are used at which point the ground control overwhelms the tie points and positions each strip to minimize control point errors on that individual strip.

The adjustment parameters for the case of all GCP are tabulated below.

Image ID	X-Offset	Y-Offset
20000704-21524	-8.4	-8.2
20000704-21526	-7.0	-5.6
20001030-14080	-16.2	-9.3
20001030-14079	0.3	2.5
20000424-12632	-4.0	-2.8
20000424-12630	-8.2	-1.9
20001030-14077	-7.5	-3.9
20001030-14078	-6.9	-3.3
20000916-13445	-3.4	-8.8
20000916-13443	-2.1	-8.0
20000927-22340	-1.7	-2.4
20000927-22339	-12.1	-9.0

The image identifications follow IKONOS practice: 4-digit year, 2-digit month, 2-digit day, some other digits, then a 5-digit sequence number. Stereo images are taken on the same orbital path, hence they are on the same date. The X (sample) and Y (line) axis adjustments are shown for each image. The adjustments are seen to be small, mostly under 10 pixels.

CONCLUSIONS

The RPC camera model has been shown to be simple and accurate. Block adjustment with RPC data is possible by combining physical parameters having the same effect on the object-image relationship into a single adjustment parameter. The resulting model improves numerical stability and user understanding of the adjustment process. The proposed block adjustment process for RPC models has been shown by simulation and numerical example to be an accurate, effective means of adjusting IKONOS images. Because RPC models can describe a variety of sensor systems, the authors believe this method is generally applicable to all satellite imaging systems with a narrow field of view, calibrated interior orientation, and good a-priori knowledge of the exterior orientation parameters.

REFERENCES

Dial, Gene (2000), RPC Data File Format. Space Imaging, QA-REF-054, Rev. B, 9/12/00.

Dial, Gene (2001). IKONOS Overview. *Proceedings of the High-Spatial Resolution Commercial Imagery Workshop*, Washington DC, March 19-22, 2001.

Dial, Gene, Laurie Gibson, and Rick Poulsen (2001), IKONOS satellite imagery and its use in automated road extraction" in Baltsavias, Gruen, and Gool, *Automatic Extraction of Man-Made objects from Aerial and Space Images (III)*, A.A. Balkema Publishers, 2001.

Grodecki, Jacek (2001), IKONOS Stereo Feature Extraction—RPC Approach. ASPRS, St. Louis, 2001.

Grodecki, Jacek and Gene Dial (2001), IKONOS Geometric Accuracy. *Proceedings of Joint International Workshop on High Resolution Mapping from Space,* Hannover, Sept 19-21, 2001.

Hu, Yong and C. Vincent Tao (2001). Updating Solutions of the Rational Function Model Using Additional Control Points for Enhanced Photogrammetric Processing. *Proceedings of Joint International Workshop on High Resolution Mapping from Space*, Hannover, Sept 19-21, 2001.

Tao, C. Vincent and Yong Hu (2001). A Comprehensive Study of the Rational Function Model for Photogrammetric Processing. *Photogrammetric Engineering & Remote Sensing,* Vol. 67, No. 12, December 2001, pp. 1347-1357.

Toutin, Thierry and Philip Cheng (2000). Demystification of IKONOS. *Earth Observation Magazine*, July 2000, pp. 17-21.

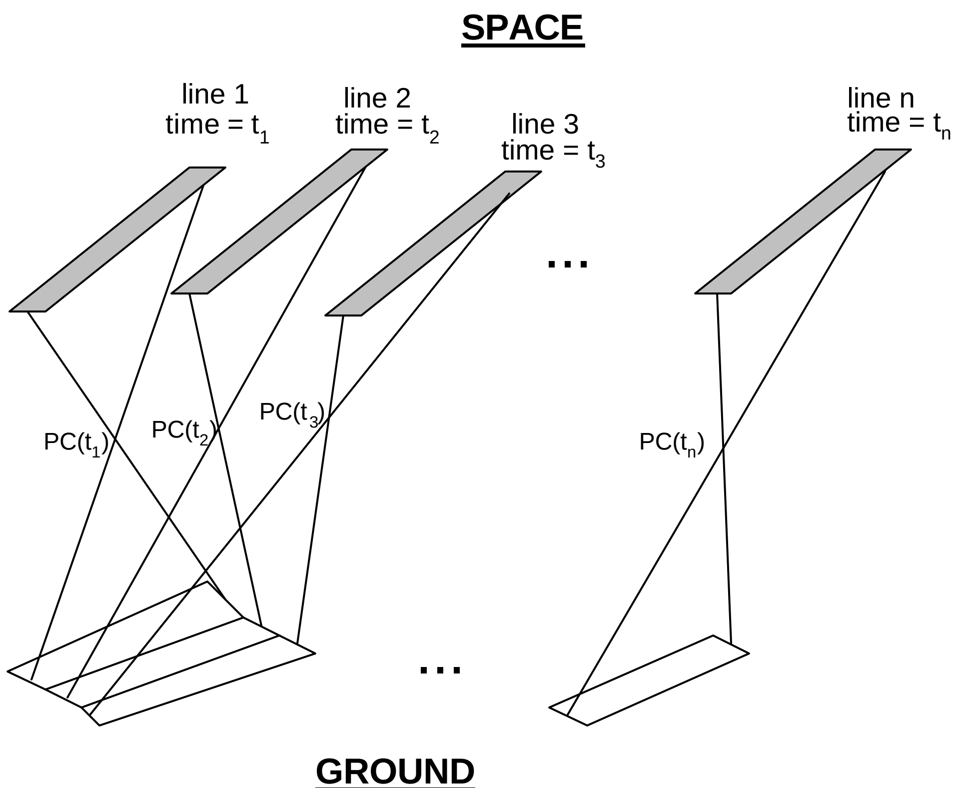

Figure 1. Exterior orientation changing as a function of time

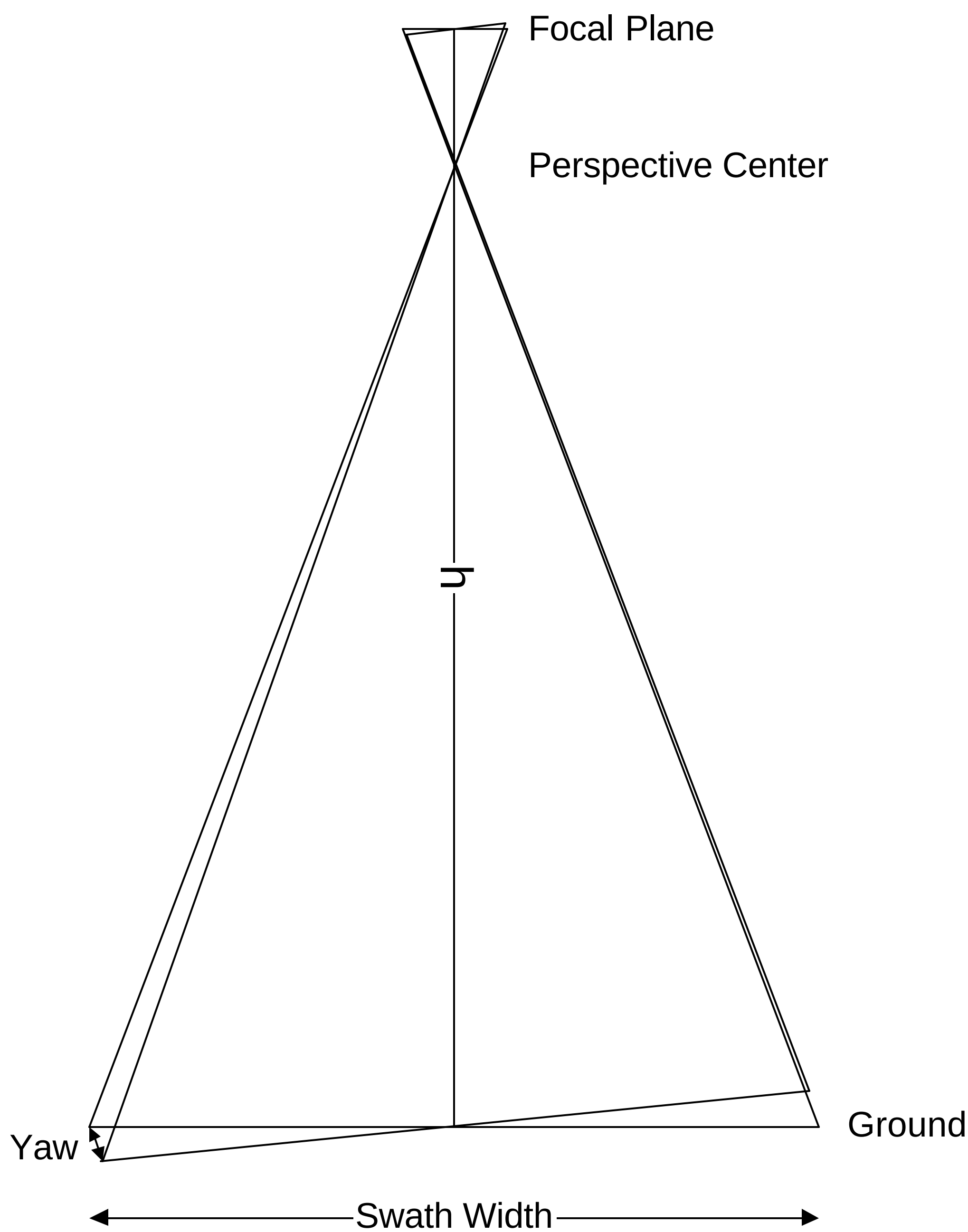

Figure 2. Effect of Yaw on Position

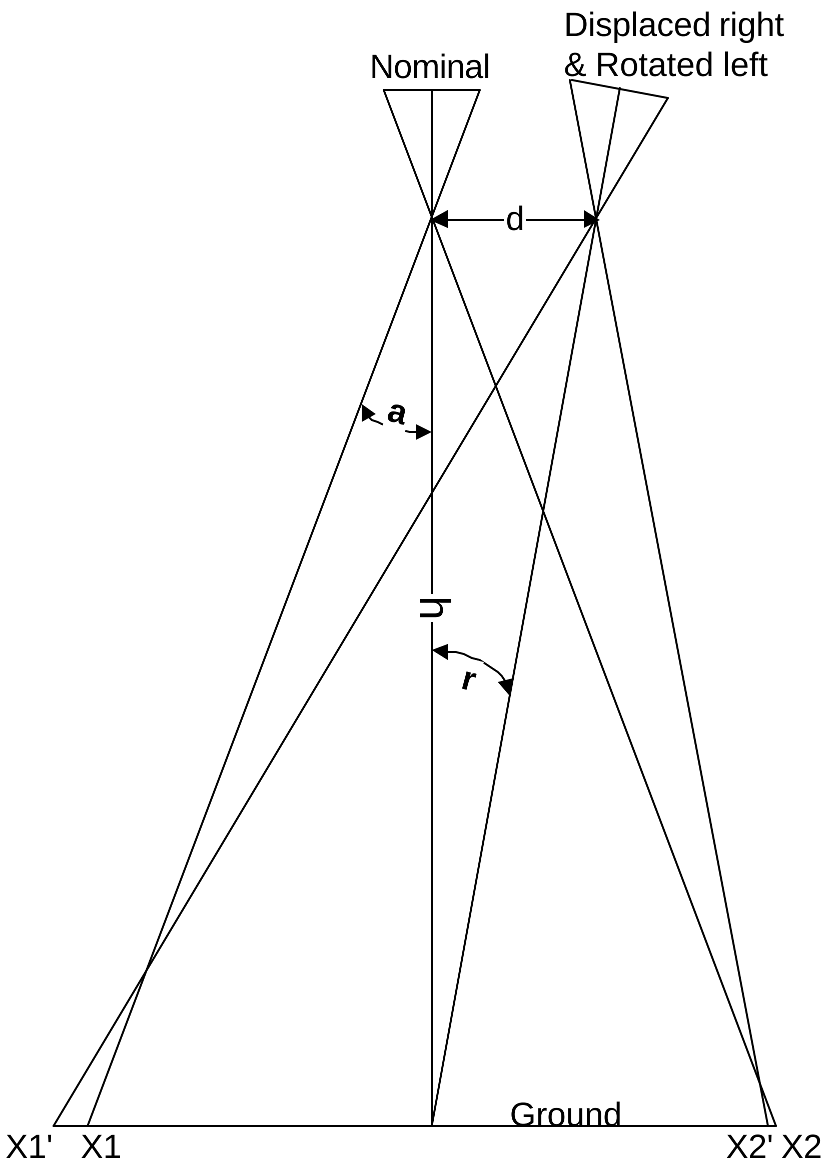

a = half-angle of the camera field of view; for IKONOS a ~ 8.3mR.
h = orbital height; for IKONOS, h ~ 680km.
r = camera roll angle, e.g., 2” ~ 9.6927E-6 radian.
d = equivalent displacement = h tan(r) = 6.593466063m.
X1 = ground coordinate of the left edge of the nominal camera,
X1 = -h tan(a) = -5644.129609
X1’ = ground coordinate of the left edge of the displaced & rotated camera,
X1’ = d – h tan(a + r) = -5644.130063
X2 = ground coordinate of the right edge of the nominal camera,
X2 = h tan(a) = 5644.129609
X2’ = ground coordinate of the right edge of the displaced & rotated camera,
X2’ = d + h tan(a - r) = 5644.129155.

Figure 3. Effect of displacement and rotation

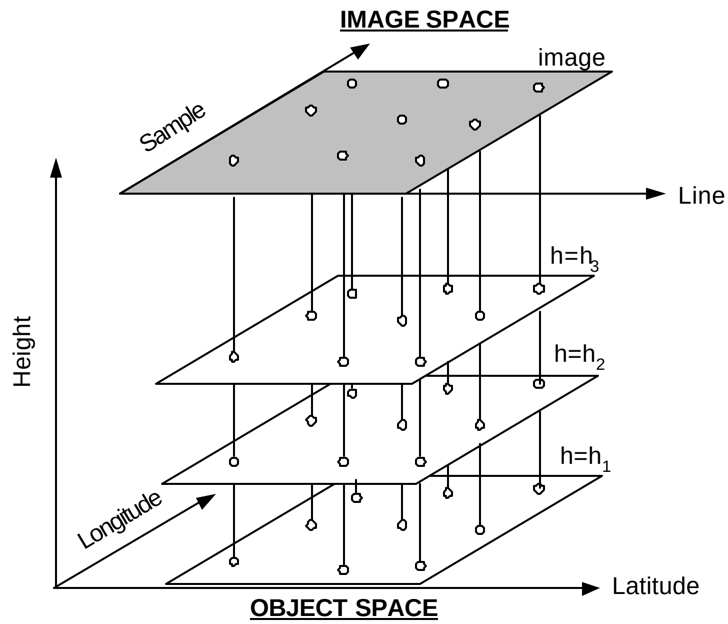

Figure 4. RPC fitting

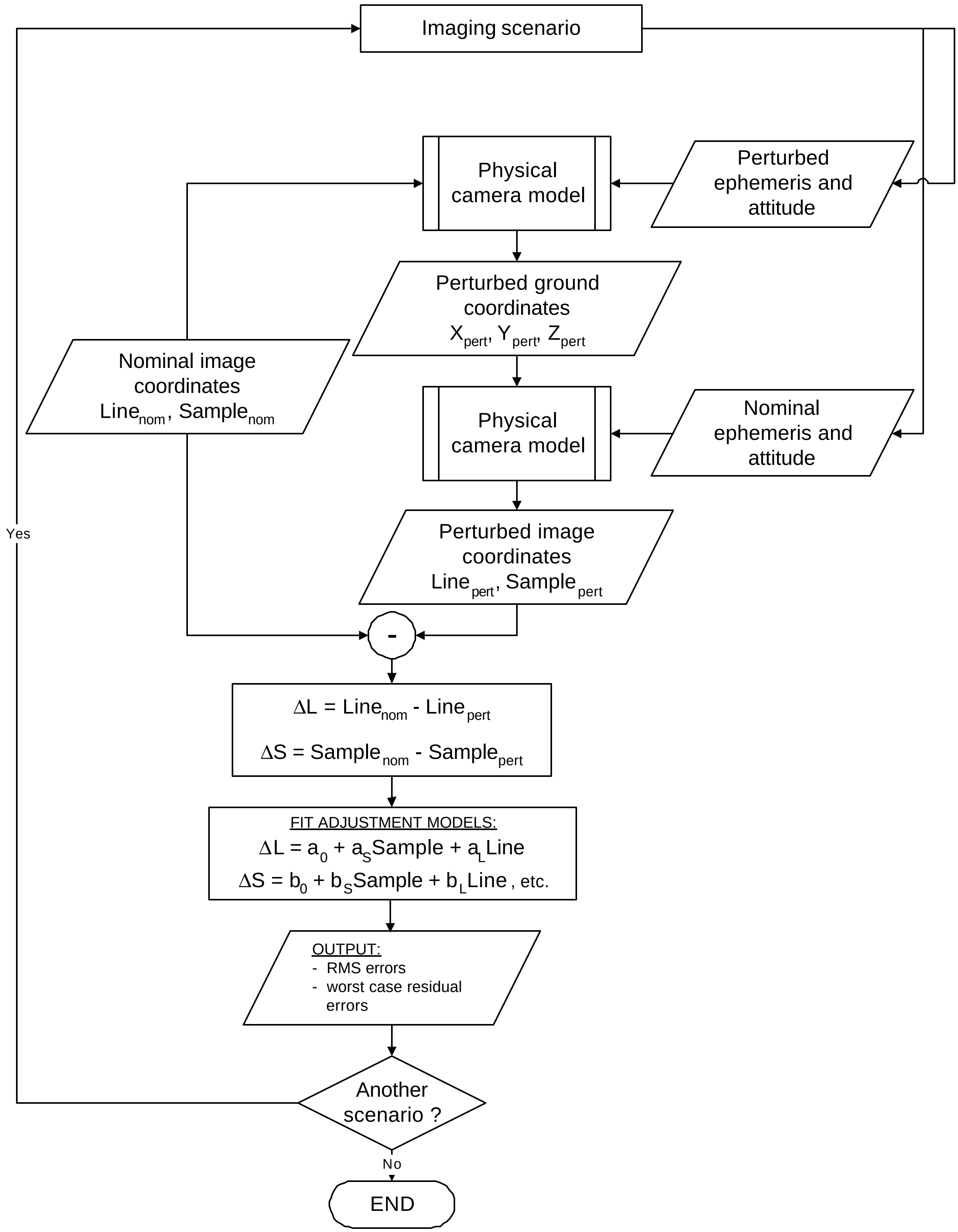

Figure 5. Perturbation Analysis of Adjustment Models

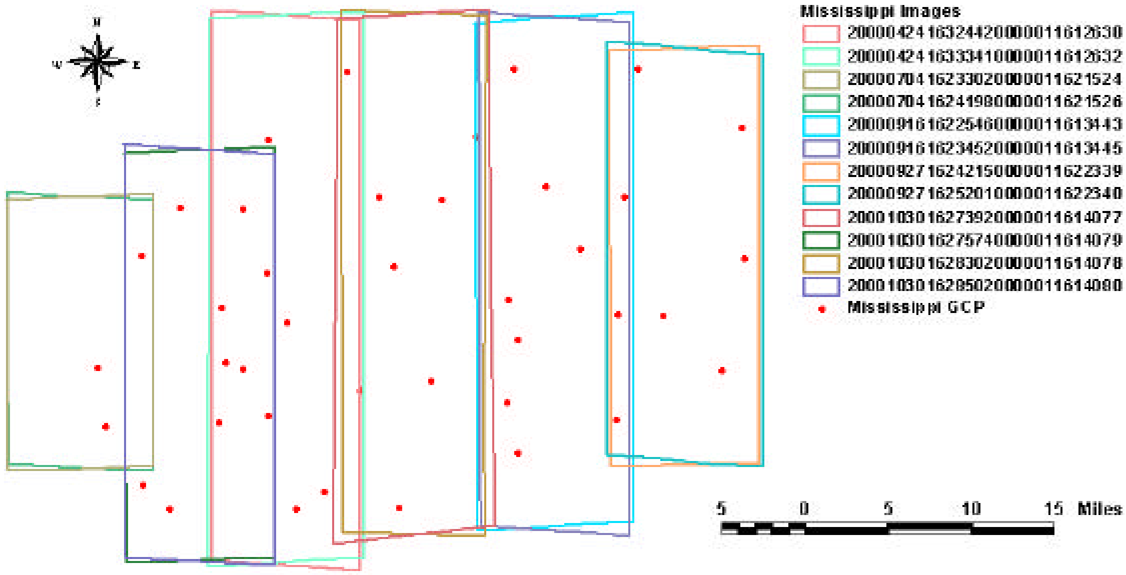

Figure 6. Stereo image strip and GCP layout for Mississippi project

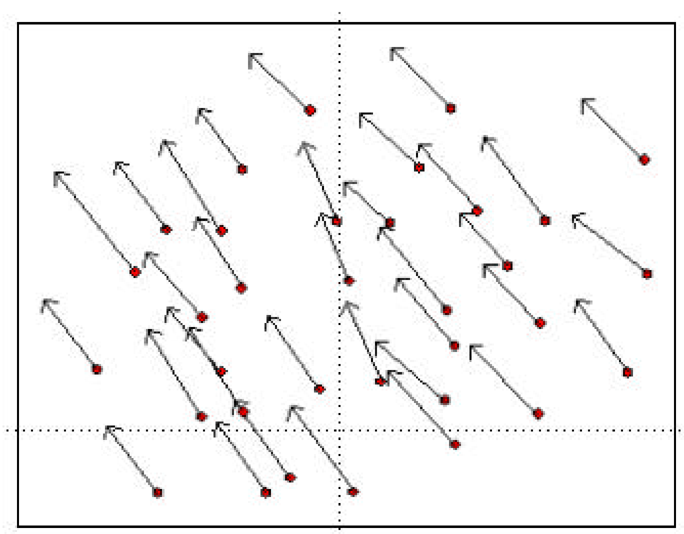

Figure 7. Residual Errors without GCP

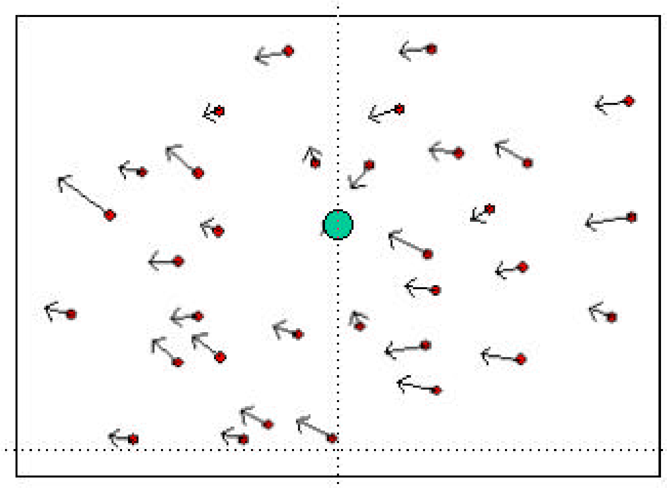

Figure 8. Horizontal errors with one GCP in center

Figure 9. Horizontal Errors with 3 GCP on West edge

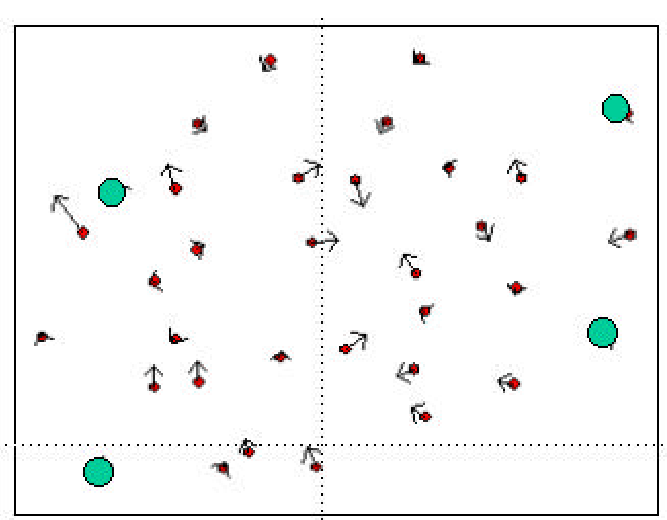

Figure 10. Horizontal Errors with 4 GCP in Corners

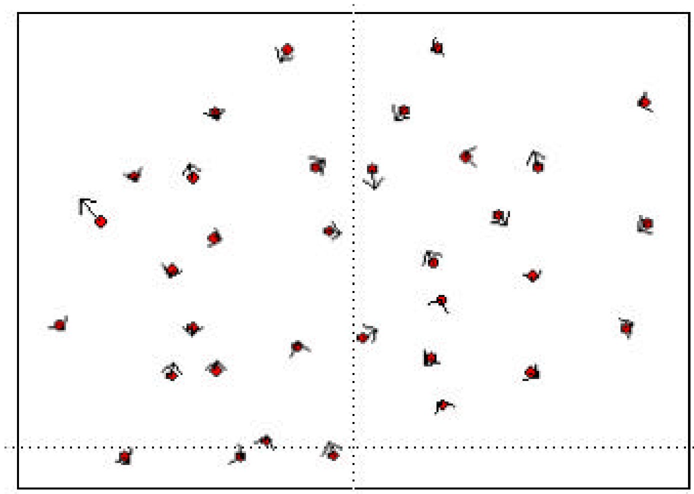

Figure 11. Horizontal errors with all GCP